I&EC research
Industrial & Engineering Chemistry Research
pubs.acs.org/IECR
Article

Simultaneous Improvement of the Processability and Mechanical Properties of Polyamide-6 by Chain Extension in Extrusion

Jianan Cai, Zhipeng Liu, Bo Cao, Xiaoxiao Guan, Shumei Liu,* and Jianqing Zhao*

Cite This: *Ind. Eng. Chem. Res.* 2020, 59, 14334−14343
Read Online

ABSTRACT: Simultaneously improving the mechanical properties and processability of polyamide-6 (PA6) by chain extension in melting extrusion is usually very difficult. To address this issue, a novel small-molecule triepoxy chain extender (D_1) is designed, synthesized, and used to modify PA6. The rheological measurements show that the shear viscosity of PA6 containing 2 wt % D_1 decreases by 52.2% compared with that of the original PA6 at a shear rate of 1000 s^{-1}, which is in the shear rate range of thermoplastic processing in the industry. This interesting result is attributed to the generation of a long-chain-branched structure of the macromolecular chains of chain-extended PA6, which reduces the power-law index and aggravates the shear-thinning behavior of the PA6 melt. In addition, the corresponding notched impact strength increases from 62.4 to 105.9 J/m. As a result, this work provides a feasible way to prepare PA6 with excellent mechanical properties and processability in industrial production.

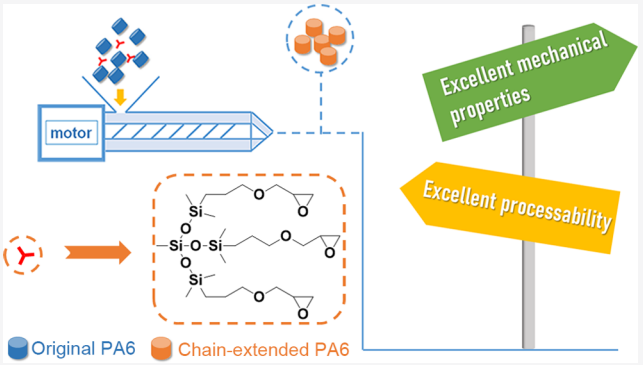

1. INTRODUCTION

Polyamide-6 (PA6) is one of the most widely used engineering thermoplastics due to its excellent overall performance. The macromolecular chains of PA6 contain many highly polar amide groups and easily absorb water, and the presence of small amounts of moisture and impurities leads to hydrolysis during high-temperature processing. As a result, the molecular weight, melt viscosity, and mechanical properties of PA6 are reduced after processing. Chain extension modification is a feasible method to compensate for the degradation of PA6 during processing.[1,2] Chain extenders can be either low-molecular-weight monomeric chemicals or polymeric materials that contain at least two functional groups capable of reacting with the amino or/and carboxyl end groups of PA6 chains.[1] The common functional groups in chain extenders are anhydride, oxazoline, epoxide, and so on.[1−4] Due to the high reactivity of the epoxy group with both the amino and carboxyl groups, epoxy compounds are one of the most common chain extenders used for PA6.[5,6] Wirasaputra et al.[7] employed a small-molecule diepoxy chain extender (BGPPO) to extend the molecular chains of PA6 in the extrusion process. The introduction of BGPPO resulted in a linear elongation of the PA6 molecular chains and thus improved the mechanical properties of PA6. However, the shear viscosity of PA6 was significantly increased over the entire shear rate range, which adversely affected the processability of PA6. In addition to the mechanical properties, processability is also an important performance factor of a given material, which not only determines the industrial production efficiency but also plays an important role in the product quality.

It is worth noting that the industrial processing of polymers often occurs at high shear rates (>100 s^{-1}), which includes processing methods such as extrusion, injection molding, and film blowing.[8] Therefore, it is crucial to improve the processability of PA6 at high shear rates. A bifunctional chain extender usually maintains the linear structure of PA6, while the introduction of a multifunctional chain extender (functionality greater than 2) can produce a long-chain-branched polymer, which is beneficial to the shear-thinning behavior of the polymer melt.[9−11] Due to the prominent shear-thinning behavior, the melt viscosity of the polymer significantly decreases at high shear rates. In other words, the utilization of a multifunctional chain extender can improve the processability of polymers at high shear rates.[9,12] Xu et al.[13] reported that the multifunctional epoxy-based chain extender KL-E4370 (functionality 9, molecular weight 6500−7000, epoxide equivalent 270−300 g/mol) significantly exacerbated the shear-thinning behavior of PA6 and decreased the shear viscosity of PA6 at the high shear region. Nevertheless, the

Received: April 21, 2020
Revised: July 17, 2020
Accepted: July 22, 2020
Published: July 22, 2020

https://dx.doi.org/10.1021/acs.iecr.0c02022
Ind. Eng. Chem. Res. 2020, 59, 14334−14343

Scheme 1. Synthesis of D_1

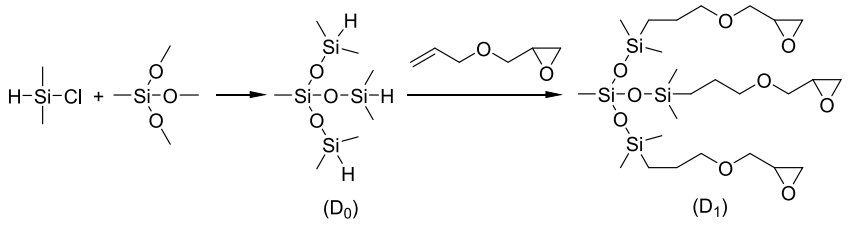

viscosity of PA6 modified by KL-E4370 was still higher than that of the unmodified PA6 at high shear rates, which might be due to the high functionality of KL-E4370. Rosu et al.[14] found that the viscosity of long-chain-branched polymers increases with the amount of branching. The higher the functionality of the chain extender, the more likely it is to produce long-chain-branched PA6 with a high branching degree and even cause PA6 cross-linking. Therefore, a suitable functionality of chain extender is crucial to the shear-thinning behavior of the chain-extended PA6. In addition, a small-molecule chain extender shows higher reactivity than a polymeric chain extender.[15] Therefore, a small-molecule chain extender with trifunctionality is expected to simultaneously improve the mechanical properties and processability of PA6 by chain extension.

In this paper, a novel small-molecule triepoxy chain extender (D_1) was synthesized from methyltrimethoxysilane, chlorodimethylsilane, and allyl glycidyl ether by a two-step method. The chain extension effect of D_1 was measured by the melt torque and mechanical properties of PA6. Rheological measurements were used to investigate the processability and structure of PA6 before and after the addition of D_1. Moreover, the chain extension effect of D_1 was also compared with a commercial chain extender Joncryl ADR-4370F. This work provides a feasible method to optimize the tradeoff between the processability and mechanical properties of PA6, which simultaneously ensures the high performance and yield of modified PA6 in industrial production.

2. EXPERIMENTAL SECTION

2.1. Materials. PA6 (general grade, TP4208), with an average molecular weight of 18 000, was obtained from Zig Sheng Industrial Co., Taiwan. Methyltrimethoxysilane, chlorodimethylsilane, allyl glycidyl ether, and chloroplatinic acid were purchased from Shanghai Aladdin Chemistry Co., China. D_1 was synthesized in our laboratory. Joncryl ADR-4370F, abbreviated as ADR in this article, was provided by BASF. ADR is a multifunctional styrene−acrylic-based polymer (functionality 5−10) with a molecular weight of 7000 and an epoxy equivalent of 285 g/mol.[16]

2.2. Synthesis of D_1. According to the literature,[17] methyltrimethoxysilane (5.44 g, 0.04 mol), ethanol (10 mL), and deionized water (5 mL) were mixed in a 250 mL three-neck round-bottom flask equipped with a magnetic stirrer, reflux condenser, and dropping funnel and stirred for 30 min under a nitrogen atmosphere in an ice bath (<5 °C). Subsequently, dimethylchlorosilane (17.03 g, 0.18 mol) was added dropwise to the above solution within 30 min under stirring. After 3 h, the above solution was acidized by a few drops of concentrated H_2SO_4 and stirred for 15 min to obtain the suspension with the intermediate (D_0) in the supernatant. Finally, after the supernatant was separated, intermediate D_0 was obtained, washed with deionized water and a saturated aqueous solution of sodium chloride, and dried overnight with anhydrous sodium sulfate (see Scheme 1). Yield: 90%. FTIR (KBr): 1061, 1119 cm^{-1} (−Si−O−Si−), 2136 cm^{-1} (−Si−H); ^1H NMR ($CDCl_3$, δ ppm): 0.07 (b, 3H), 0.21 (a, 18H), 4.73 (c, 3H).

Allyl glycidyl ether (4.56 g, 0.04 mol), toluene (50 mL), and Speier catalyst (0.25 mL, 5 mg/mL) were added to a 100 mL three-neck round-bottom flask equipped with a magnetic stirrer, reflux condenser, and dropping funnel and heated to 60 °C under a nitrogen atmosphere. Afterward, D_0 (2.69 g, 0.01 mol) was added dropwise to the above solution within 30 min under stirring. The reaction was carried out for 8 h at 80 °C. Finally, the solvent was removed by rotary evaporation, and the crude product was dried in a vacuum oven to obtain product D_1 (see Scheme 1). Yield: 84%. FTIR (KBr): 1051, 1109 cm^{-1} (−Si−O−Si−), 911 cm^{-1} (epoxy ring); ^1H NMR ($CDCl_3$, δ ppm): 0.04 (d, 3H), 0.08 (e, 18H), 0.55 (f, 6H), 1.61 (g, 6H), 2.59 (k, 6H, *trans*), 2.78 (k′, 6H, *cis*), 3.13 (j, 3H), 3.42 (h, 6H), 3.44 (i′, 6H, *cis*), 3.67 (i, 6H, *trans*). MS: m/z = 633.28 ($[M + Na^+]$).

2.3. Processing. The critical mole fraction of D_1 for gelation, α_c, was estimated according to the following equation

$$\alpha_c = \frac{1}{f-1} \tag{1}$$

where f is the chain extender functionality.[18,19] D_1 has a functionality of 3, and α_c is calculated as 0.5. The molecular weight of D_1 is 610.28 and the average molecular weight of PA6 is 18 000, implying that the critical weight faction of D_1 for gelation is 3.3 wt %. The functionality of ADR is 5−10 and its average molecular weight is 7000, implying that the critical weight faction of ADR for gelation is 4.5 wt %. Therefore, the added amount of D_1 and ADR is below 2.0 wt % to avoid the gelation, and the compositions are listed in Table 1. Before processing, PA6, D_1, and ADR were dried for 6 h at 90 and 80 °C in vacuum, respectively. According to the compositions, PA6 and D_1 or ADR were extruded in a 26 mm corotating twin-screw extruder (L/D = 40) from Labtech Engineering (Thailand). The extruder was configured with ten heating zones, and the extrusion was carried out at zone temperature

Table 1. Compositions and Code Names of the Samples

samples	compositions (wt %)		
	PA6	D_1	ADR
PA6	100	0	0
PA6/D_1-0.5	99.5	0.5	0
PA6/D_1-1.0	99.0	1.0	0
PA6/D_1-1.5	98.5	1.5	0
PA6/D_1-2.0	98.0	2.0	0
PA6/ADR-1.0	99.0	0	1.0
PA6/ADR-2.0	98.0	0	2.0

https://dx.doi.org/10.1021/acs.iecr.0c02022
Ind. Eng. Chem. Res. 2020, 59, 14334−14343

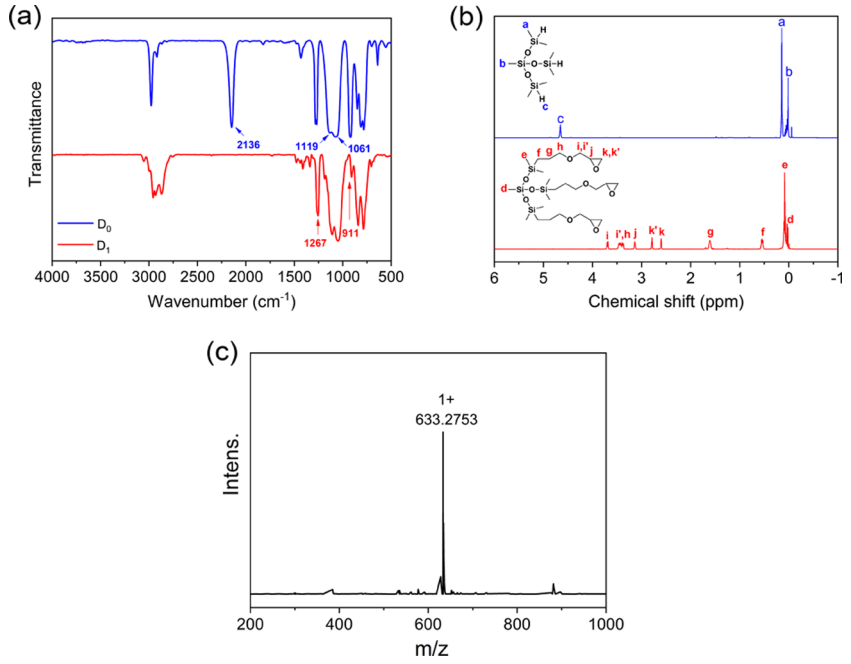

Figure 1. (a) FTIR spectra of D_0 and D_1, (b) ^1H NMR spectra of D_0 and D_1, and (c) MS spectrum of D_1.

profiles of 180−220−230−230−230−230−230−230−230−220 °C. The extrusion was conducted at a 180 rpm screw speed, producing a continuous approximately 3 mm diameter strand with a 6 kg/h output, water-cooled immediately on exit in a 1.5 m long trough, and then pelletized. After being dried in vacuum at 90 °C for 6 h, most extruded pellets were injection-molded into various types of specimens using an EC75-NII injection molding machine (Toshiba, Japan). Some pellets were molded into disks with a diameter of 25 mm and a thickness of 1 mm to test the rheological properties.

2.4. Measurements. Fourier transform infrared (FTIR) spectra were recorded with a Vertex70 spectroscope (Bruker, Germany). ^1H NMR spectra were collected with an Avance400 NMR spectrometer (Brucker, Germany) using $CDCl_3$ as a solvent. Mass spectrometry (MS) spectrum was obtained with a maXis impact mass spectrometer (Brucker, Germany). The epoxy equivalent weight of D_1 was determined by the hydrochloric acid−acetone solution method described in the literature.[20] Dried PA6 pellets with various amounts of the chain extender were added to the mixing chamber of a Haake Rheomix 600 equipped with a roller rotor to test the melt torque. The processing was performed at a rotor speed of 40 rpm at 230 °C. After the melt torque approached a stable value, the sample was removed from the mixing chamber and used for group content testing. The amino and carboxyl group contents of PA6 molecular chains were analyzed according to the Waltz−Taylor titration method.[21] The rheological properties were measured at 230 °C using an AR-G2 rheometer (TA Instruments). Time sweep tests were conducted at a 1 Hz frequency over 1000 s. The shear viscosity was obtained at the shear rate range of 1−1000 s^{-1}. Dynamic oscillatory tests were performed in the linear viscoelastic region with an angular frequency ranging from 0.1 to 628 rad/s. The tensile and flexural strengths were tested using a Z010 universal tester (Zwick/Roell, Germany) according to the standards ASTM D-638 and ASTM D-790, respectively. The notched Izod impact strength was measured using a Zwick5113 impact pendulum machine (Zwick Roell, Germany) in accordance with the ASTM D-256 standard. Differential scanning calorimetry (DSC) measurements were carried out under a nitrogen atmosphere with a DSC-204FI (Netzsch, Germany) ranging from room temperature to 260 °C at a rate of 10 °C /min. Prior to the X-ray diffraction (XRD) experiments, the samples were heated to 230 °C and maintained at 230 °C for 5 min to remove the thermal history of these samples. Then, the samples were quenched in liquid nitrogen and subsequently maintained at room temperature for 24 h. XRD analysis of the original and extended PA6 was performed using a D8ADVANCE wide-angle X-ray diffractometer (Brucker, Germany) at room temperature. XRD data were collected from 10 to 30° of 2θ.

3. RESULTS AND DISCUSSION

3.1. Characterization of D_1. The chemical structure of D_1 is characterized by FTIR, ^1H NMR, and MS spectra (Figure 1). The FTIR spectrum of D_1 is compared with that of D_0 in Figure 1a. The characteristic absorption peaks of Si−O−Si appear at approximately 1060 and 1110 cm^{-1}, and the characteristic absorption peak of Si−C appears at 1267 cm^{-1} in the IR spectra of D_0 and D_1. The IR spectrum of D_0 shows a characteristic Si−H absorption peak at 2136 cm^{-1}. After the hydrosilylation reaction of D_0 with allyl glycidyl ether, the characteristic peak of Si−H disappears, while the characteristic peak of the epoxy ring appears at 911 cm^{-1} in the IR spectrum of D_1, suggesting that D_0 has been completely reacted.

The ^1H NMR spectra of D_0 and D_1 are shown in Figure 1b. The peak of the proton in the Si−H group of D_0 is located at 4.73 ppm in the ^1H NMR spectrum, but it disappears for D_1 after the hydrosilylation reaction, further indicating that D_0 has been completely reacted. The formation of D_1 is confirmed by the characteristic peaks of the protons in the epoxy ring that appear at 2.59 ppm (k, *trans*), 2.78 ppm (k′, *cis*), and 3.13 ppm (j). The peaks at 0.04 ppm (d) and 0.08 ppm (e) are attributed to the protons in Si−CH_3. The chemical shift of the protons in the −CH_2−CH_2−CH_2−O− group appears as a triplet at 3.42 ppm (h), a multiplet at 1.61 ppm (g), and a triplet at 0.55 ppm

https://dx.doi.org/10.1021/acs.iecr.0c02022
Ind. Eng. Chem. Res. 2020, 59, 14334−14343

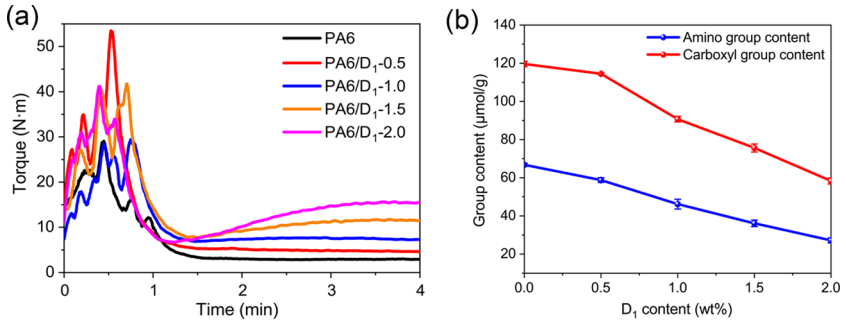

Figure 2. (a) Torque versus time at different D_1 loadings at 230 °C and 40 rpm and (b) amino and carboxyl group contents of PA6 at different D_1 loadings after 4 min of mixing.

(f). Additionally, the chemical shift at 3.44 ppm (i′, *cis*) and 3.67 ppm (i, *trans*) in the ^{1}H NMR spectrum of D_1 belongs to the protons in CH_2 of the −O−CH_2−epoxy ring group.

The MS spectrum of D_1 shows an $[M + Na^+]$ ion peak at *m*/*z* 633.28 (molecular formula = $C_{25}H_{54}O_9Si_4$), which is consistent with the theoretical molecular weight of D_1 (610.28). In addition, the epoxy equivalent weight of D_1 is determined to be 203 g/mol by the hydrochloric acid−acetone solution method. The above results confirm that the designed D_1 is successfully synthesized.

3.2. Chain Extension Reaction between D_1 and PA6. The epoxy groups of the D_1 molecule can react with the amino and carboxyl groups of PA6 to achieve elongation or branching of the PA6 macromolecular chains during processing. To evaluate the chain extension effect of D_1, the melt torque and the amino and carboxyl group contents of PA6 were measured, and the results are shown in Figure 2 and Table S1 in the Supporting Information.

The melt torque measurement, a method to characterize the rheological property of polymers at low shear rates,[22] was used to evaluate the melt processing of PA6 and the result of the reaction between PA6 and D_1. After complete melting, the torque of the original PA6 reaches and maintains equilibrium, as shown in Figure 2a. In contrast, in the extended PA6, the torque begins to increase after the melting period and reaches equilibrium after approximately 4 min of mixing. The equilibrium torque value of PA6 gradually increases with the addition of D_1. When the amount of D_1 is 2.0 wt %, the equilibrium torque value of PA6 reaches 15.3 N·m, which is nearly 6 times higher than that of the original PA6, confirming the occurrence of a chain extension reaction. The chain extension reaction increases the molecular weight of PA6, thus increasing the friction and entanglement between the macromolecular chains and resulting in the observed increase in the melt torque.[23] The results also indicate that D_1 displays high reactivity from the start of melt processing.

The concentrations of both amino and carboxyl groups of the PA6 macromolecules decrease after adding D_1, and the former decreases more than the latter, indicating that the reactivity of the epoxy groups is higher with amino groups than the reactivity with carboxyl groups (Figure 2b). The amino group content in PA6/D_1-2.0 decreases to 27.2 from 66.8 μmol/g in PA6, and the carboxyl group content decreases to 58.3 from 119.6 μmol/g. Compared with the contents in the original PA6, the amino and carboxyl group contents of PA6/D_1-2.0 are decreased by 59.3 and 51.2%, respectively. The above results also indicate that the chain extension reaction between D_1 and PA6 indeed occurs.

3.3. Rheological Behavior. An enhancement in the melt torque of polymers is usually correlated with a deterioration in processability. Considering the pseudoplasticity of the polymer melt, in which the apparent viscosity declines as the shear rate increases, it is possible to improve the processability at a high shear rate. Therefore, it is important to evaluate the effect of D_1 on the processability of PA6 at different shear rates.

First, isothermal time sweep experiments in the dynamic oscillatory mode were conducted to test the melt stability of the original and extended PA6. Figure 3 shows their complex

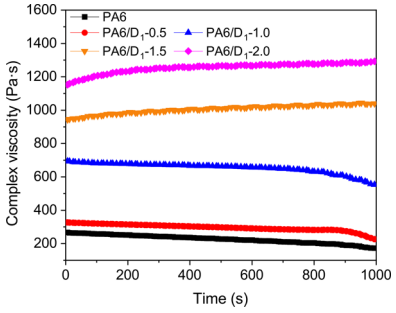

Figure 3. Complex viscosity as a function of time for the original and extended PA6.

viscosity as a function of time at 230 °C and a frequency of 1 Hz. A decrease in the complex viscosity of the original PA6, PA6/D_1-0.5, and PA6/D_1-1.0 is observed, originating from the PA6 degradation at the melt temperature over time. Interestingly, the complex viscosity of PA6/D_1-1.5 and PA6/D_1-2.0 increases slowly over time, which may be attributed to an ongoing chain extension reaction in the rheometer.

To evaluate the processability of the original and extended PA6 at different shear rates, the shear viscosity (η) was plotted as a function of the shear rate ($\dot{\gamma}$) for the original and extended PA6 with various D_1 contents. As shown in Figure 4, the shear viscosity of PA6 shifts to a higher value with the addition of D_1 at low shear rates (<100 s^{-1}), which is consistent with the melt torque results shown in Figure 2a. With increasing D_1 content, the shear-thinning behavior of the PA6 melt becomes more obvious. The prominent shear-thinning behavior can result in a rapid decrease in the melt viscosity of PA6 as the shear rate increases.[9,12] As shown in Figure 4, the shear viscosity of the extended PA6 is very close to that of the original PA6 in the shear rate range of 100−500 s^{-1}. When the shear rate is higher than 500 s^{-1}, the viscosity of PA6 gradually decreases with the addition of D_1. With the added amount of 2.0 wt % D_1, the viscosity of PA6 at the shear rate of 1000 s^{-1} decreases by

https://dx.doi.org/10.1021/acs.iecr.0c02022
Ind. Eng. Chem. Res. 2020, 59, 14334−14343

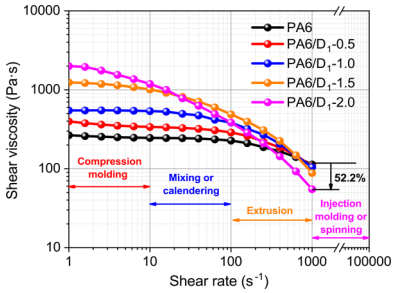

Figure 4. Shear viscosity curves of the original and extended PA6.

52.2% compared with that of the original PA6. The greater shear thinning of the extended PA6 provides a lower viscosity at high shear rates than that of the original PA6. As an important rheological parameter, the shear viscosity is commonly used to evaluate the processability of polymers, and a high shear viscosity is related to poor processability.[24,25] The above results imply that the introduction of D_1 does not deteriorate the processability, and it even improves the processability of PA6 at high shear rates (>100 s^{-1}), which is the common shear range for industrial processing such as extrusion (100−1000 s^{-1}) and injection molding and spinning (>1000 s^{-1}).[8,26] Therefore, the introduction of D_1 ensures good processability of PA6 in industrial processing and the efficiency of industrial production.

In addition, other rheological parameters of the original and extended PA6 were calculated from Figure 4 by the Carreau equation (eq 1) and power-law equation (eq 2). In eq 1, η_0 is the zero-shear viscosity, λ is the relaxation time, $\dot{\gamma}$ is the shear rate, a is a parameter. In eq 2, $\eta(\dot{\gamma})$ is the shear viscosity, $\dot{\gamma}$ is the shear rate, K is the consistency coefficient, and n is the power-law index. The calculated results care listed in Table 2.

$$\eta = \frac{\eta_0}{[1 + (\lambda\dot{\gamma})^2]^{1-a/2}} \quad (2)$$

$$\eta(\dot{\gamma}) = K\dot{\gamma}^{n-1} \quad (3)$$

Table 2. Rheological Parameters of the Original and Extended PA6

samples	η_0 (Pa·s)	λ (s)	n^a (power-law index)
PA6	2.55×10^2	1.1×10^{-2}	0.74
PA6/D_1-0.5	3.71×10^2	1.8×10^{-2}	0.63
PA6/D_1-1.0	5.55×10^2	2.6×10^{-2}	0.50
PA6/D_1-1.5	1.31×10^3	1.4×10^{-1}	0.34
PA6/D_1-2.0	1.99×10^3	3.1×10^{-1}	0.22

[a] n is calculated at the shear range of 100−1000 s^{-1}.

The zero-shear viscosity of PA6 increases from 2.55×10^2 to 1.99×10^3 Pa·s after modification with 2.0 wt % D_1, indicating the occurrence of chain extension. The chain extension reaction increases the molecular weight of PA6 and the entanglement between macromolecular chains, consequently increasing the viscosity of the polymer melt.[27,28] In addition, an increase in the molecular chain entanglement density leads to longer relaxation time,[29] as shown in Table 2. The power-law index of the extended PA6 is smaller than that of the original PA6 and declines with increasing D_1 loading, which indicates that the melt viscosity of the extended PA6 is more sensitive to the shear rate, suggesting the more obvious pseudoplastic behavior.[30]

According to the above results, the addition of D_1 significantly changes the rheological properties of PA6. The rheological properties of polymers are closely related to their molecular structure.[31,32] Due to the multifunctionality of D_1, the reaction between D_1 and PA6 not only results in the linear elongation of the molecular chains but also may produce branched structures. The relevant reaction mechanism and the possible molecular structures formed during the reaction are summarized in Figure 5.

First, the coupling reaction occurs between two epoxy groups in one molecule of D_1 and two macromolecular chains of PA6, leading to chain extension. Here, the molecular structure of PA6 is still linear. Second, a star-shaped molecule with three arms is formed after the reaction of three PA6 macromolecules with one D_1 molecule, as shown in Figure 5b. According to Figure 5c, the reaction of the PA6 chains with more than two D_1 molecules can generate other complex structures, such as H-shaped, hyperbranched treelike, or cross-linked structures. In other words, the incorporation of D_1 may change the linear structure of PA6 macromolecules and induce more diverse long-chain-branched structures.

Interestingly, based on the above results, the extended PA6 possesses the following characteristics of polymers with long-chain branches: (1) long relaxation time, (2) high zero-shear viscosity, and (3) high shear thinning sensitivity. The existence of long-chain branches increases the molecular chain entanglement density and obstructs the movement of molecular chains, thus increasing the relaxation time and the viscosity of the materials at lower shear rates.[12] However, at higher shear rates, the elongation of the molecular conformations and the disentanglement of the branches result in an evident shear-thinning behavior and a lower viscosity of long-chain-branched polymers.[12,33,34] Therefore, the addition of D_1 does not exert a negative impact on the processability of PA6 in industrial production; instead, the long-chain branches generated in the extended PA6 lead to a lower shear viscosity and better processability. To confirm this viewpoint, other rheological properties must be further investigated.

In addition to shear viscosity, the storage modulus and loss angle are even more sensitive to long-chain-branched structures. Figure 6a shows the storage modulus curves of the original and extended PA6 plotted as a function of the frequency. The storage modulus of a linear polymer follows a well-known frequency dependence at low frequencies, i.e., $G' \propto \omega^2$, which means that the terminal slope of the curve is 2 for linear PA6, which is related to the terminal relaxation of molecules.[35,36] The terminal slopes of the curves from Figure 6a were calculated as shown in Table 3. With the addition of D_1, the terminal slope decreases from 1.67 (original PA6) to 0.98 (PA6/D_1-2.0). The original PA6 and PA6/D_1-0.5 samples exhibit typical terminal behavior, indicating mostly linear molecular structures. The terminal slopes of the corresponding curves of the other three samples are much lower than 2 at low frequencies and thus deviated from the typical terminal behavior, suggesting that their relaxation process occurs at lower frequencies and takes longer. The longer relaxation process is related to the presence of long-chain branches, which increases the entanglement of molecular chains and prevents molecular relaxation.[37] This indicates that the reaction between PA6 and D_1 results in the formation of long-chain-branched structures, as shown in Figure 5.

https://dx.doi.org/10.1021/acs.iecr.0c02022
Ind. Eng. Chem. Res. 2020, 59, 14334−14343

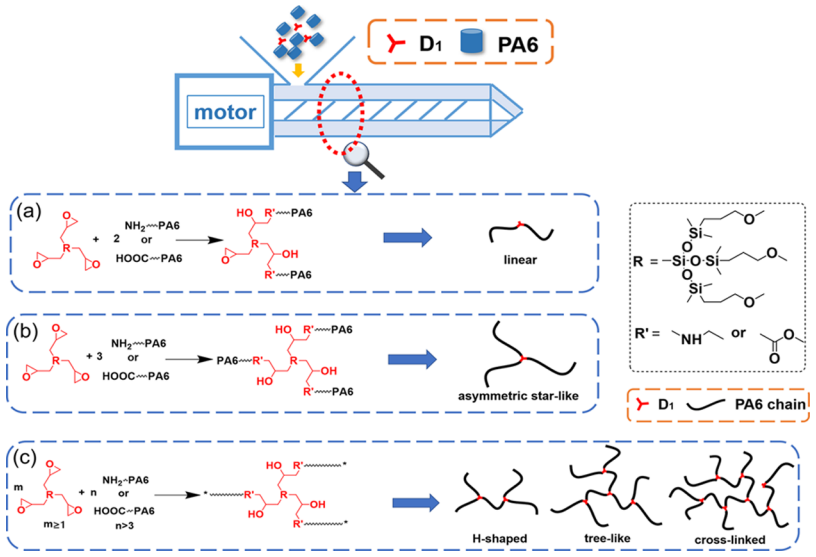

Figure 5. Mechanism of the reaction between D_1 and PA6.

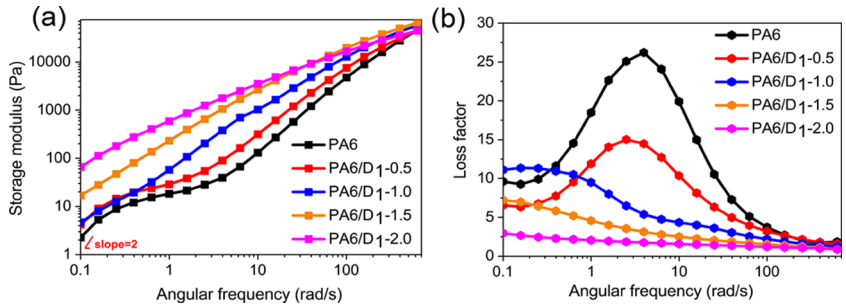

Figure 6. (a) Storage modulus curves of the original and extended PA6 and (b) loss factor curves of the original and extended PA6.

Table 3. Terminal Slope of Elastic Modulus of the Original and Extended PA6

samples	the terminal slope of G'
PA6	1.67
PA6/D_1-0.5	1.63
PA6/D_1-1.0	1.13
PA6/D_1-1.5	1.03
PA6/D_1-2.0	0.98

According to the loss factor ($\tan\delta$) curves depicted in Figure 6b, the original PA6 possesses the highest loss factor peak, and its corresponding value is higher than that of the extended PA6 over the entire frequency range. The loss factor value of the extended PA6 decreases, and the peak shifts progressively toward the lower frequencies with the addition of D_1. No peak is observed on the tan δ curves of PA6/D_1-1.5 and PA6/D_1-2.0. Generally, the value of tan δ decreases, and the plateau of the tan δ curve broadens as the long-chain branching level increases.[38−40] Therefore, the above results again indicate the formation of long-chain-branched structures after the reaction between PA6 and D_1.

Based on the above results and the discussion, D_1 induces the formation of long-chain branches and has a significant influence on the rheological behavior of PA6. The generation of long-chain branches improves the shear-thinning behavior of PA6, which positively influences the processability of PA6 at high shear rates.

3.4. Crystallization Properties of the Original and Extended PA6. As a semicrystalline polymer, the crystallization properties of PA6 play an important role in the mechanical properties. Therefore, it is crucial to investigate the effect of added D_1 on the crystallization properties of PA6. The melting and crystallization curves of PA6 with different D_1 contents via DSC measurements are illustrated in Figure 7. The data from the nonisothermal crystallization tests of the original and extended PA6 are summarized in Table S2 in the Supporting Information. The melting peak temperature (T_m^P) of PA6 remains unchanged after the addition of D_1. Compared with the crystallization peak temperature (T_c^P) of the original PA6, T_c^P of the extended PA6 shifts to a lower temperature, indicating that the PA6 crystallization process requires higher activation energy after the addition of D_1. Chain extension modification leads to an increase in the molecular weight, the formation of long-chain branches, and an increase in the molecular entanglement. The molecular entanglement and the steric effect generated by long-chain branches delay the segment movement and arrangement of the PA6 molecular chains during crystallization.[41] In addition, the introduction of D_1 decreases the crystallinity of PA6, as shown in Table S2 in the Supporting Information. When the added amount of D_1 is 2.0 wt %, the crystallinity of PA6/D_1-2.0 is reduced to 17.4 from 26.3% of the original PA6.

Moreover, the crystal structures of the original and extended PA6 were detected by XRD analysis, and their XRD patterns are shown in Figure 7c. According to the previous literature,[42,43] there are several kinds of crystalline forms of

https://dx.doi.org/10.1021/acs.iecr.0c02022
Ind. Eng. Chem. Res. 2020, 59, 14334−14343

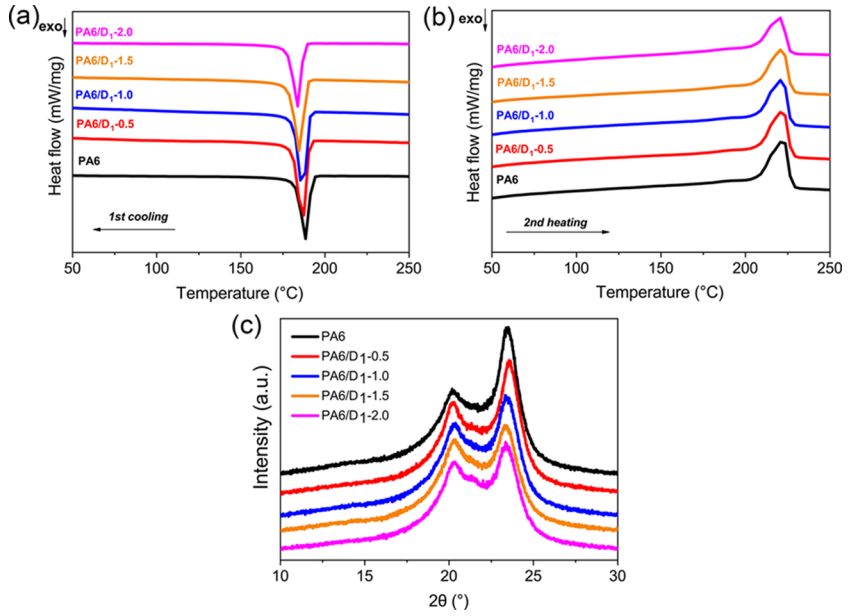

Figure 7. (a) Crystallization curves of the original and extended PA6, (b) melting curves of the original and extended PA6, and (c) XRD curves of the original and extended PA6.

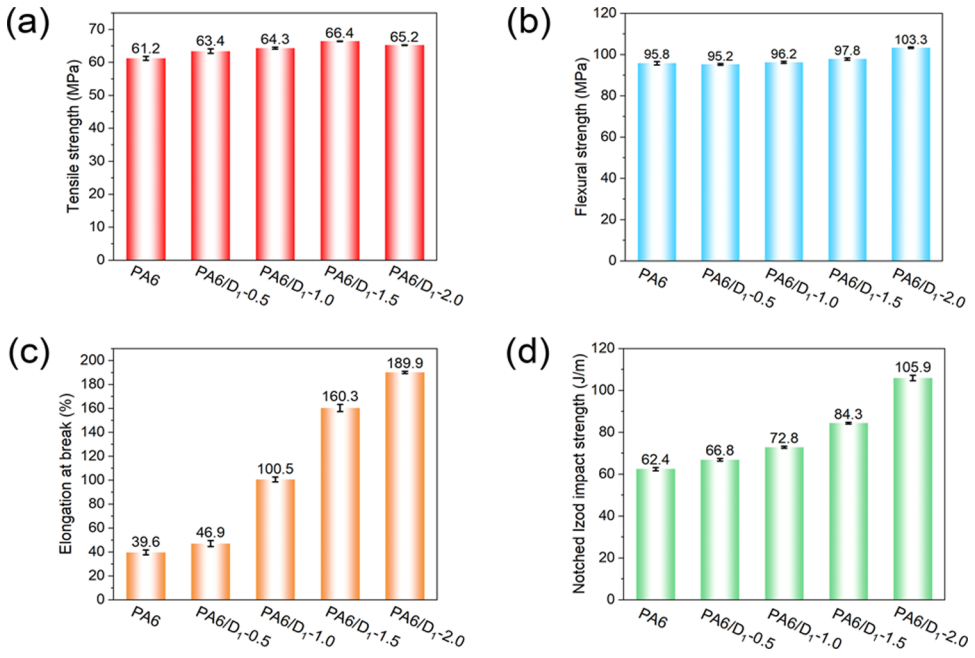

Figure 8. Mechanical properties of the original and extended PA6.

PA6, and α and γ are common crystalline forms. As shown in Figure 7c, the crystalline structure of the original PA6 is dominated by the α form crystal phase, with two characteristic peaks at approximately 20.5° (200 reflection) and 24° (002 + 202 reflections).[44,45] The extended PA6 has almost the same pattern as the original PA6, revealing that the chain extension modification has no effect on the crystal form of PA6.[46] The DSC and XRD results indicate that an increase in the molecular weight and the formation of long-chain branches reduce the crystallization capability of PA6 without changing its crystalline structure.

3.5. Mechanical Properties of the Original and Extended PA6. Figure 8 shows the mechanical properties of the original and extended PA6. The tensile and flexural strengths, which represent the rigidity of PA6, are not significantly affected by the incorporation of D_1. The elongation at break of the extended PA6 is notably improved compared with that of the original PA6, and the sample PA6/D_1-2.0 has the highest value (189.9%), which is approximately 4.8 times higher than that of the original PA6. In addition to the elongation at break, the notched impact strength is also used to evaluate the toughness of PA6. As seen in Figure 8, the effect of D_1 on the notched impact strength is similar to its effect on the elongation at break. Sample PA6/D_1-2.0 exhibits the highest notched impact strength (105.9 J/m), which is 69.7% higher than that of the original PA6. As previously mentioned, the reaction between PA6 and D_1 increases the molecular weight and results in the generation of long-chain

https://dx.doi.org/10.1021/acs.iecr.0c02022
Ind. Eng. Chem. Res. 2020, 59, 14334−14343

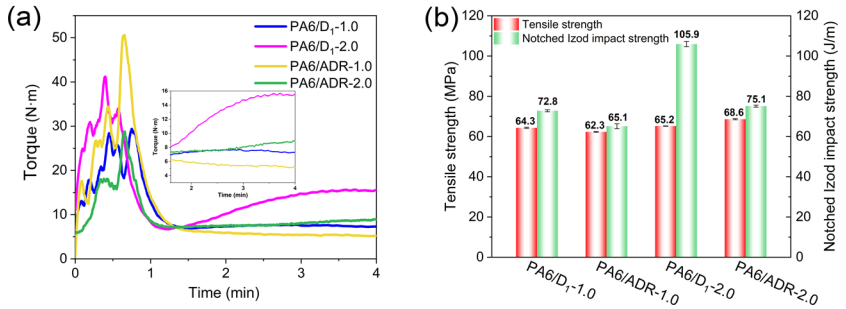

Figure 9. Comparison of the chain extension effect between D_1 and ADR.

branches, which increases the amount of molecular chain entanglement. According to the theory of polymer strength, an increase in the entanglement point, which acts as a physical cross-linking point between molecules, can increase the interaction between molecules and reduce molecular slippage.[47,48] Consequently, when subjected to external force, more stress may be transferred within the system and PA6 can withstand a larger load, accordingly increasing the mechanical strength of PA6. According to the results of DSC experiments, the crystallinity of PA6 decreases after chain extension by D_1, which results in a decrease in the rigidity but an increase in PA6 toughness. A decrease in the crystallinity allows the cracks to propagate more easily in the crystallite, which explains the increase in the toughness. Consequently, the addition of D_1 to PA6 results in improved mechanical properties, especially toughness.

3.6. Comparison of the Chain Extension Effect between D_1 and ADR. The chain extension effect of D_1 was also compared with a commercial chain extender ADR. Figure 9 shows the melt torque versus time, tensile strength, and notched Izod impact strength of PA6 with 1.0 and 2.0 wt % D_1 or ADR. As shown in Figure 9a, the torque of the extended PA6 begins to increase after the melting period, which is due to the chain extension reaction. With the same added amount, the torque of PA6/D_1 is higher than that of PA6/ADR after the melting period, exhibiting a greater chain extension effect. The torque of PA6 added with 2.0 wt % D_1 reaches equilibrium after approximately 4 min of mixing. However, after 4 min of mixing, the torque of PA6 added with 2.0 wt % ADR still exhibits an upward trend, indicating that the chain extension reaction between PA6 and ADR is still in progress. Compared with ADR, the reaction rate of D_1 with PA6 is faster, which may be due to its lower molecular weight. As shown in Figure 9b, the tensile strength of PA6 is not significantly affected by the incorporation of D_1 or ADR. Both D_1 and ADR can improve the impact strength of PA6, and D_1 exhibits a more marked improvement. The notched impact strength of PA6/D_1-1.0 is 11.8% higher than that of PA6/ADR-1.0, and the notched impact strength of PA6/D_1-2.0 is 41.0% higher than that of PA6/ADR-2.0. The above results indicate that D_1 has a higher reactivity and a greater chain extension effect than ADR.

4. CONCLUSIONS

In this article, a novel trifunctional chain extender D_1 was successfully synthesized and used to modify PA6. The equilibrium torque value of the PA6/D_1-2.0 melt was nearly 6 times larger than that of the original PA6, which implied the occurrence of a chain extension reaction. Due to the trifunctionality of D_1, long-chain branches were simultaneously formed along with the chain extension reaction, leading to more pronounced non-Newtonian flow characteristics, and the power-law index of the PA6/D_1-2.0 melt decreased to 0.22 from 0.74 of the original PA6. In addition, the shear viscosity of PA6/D_1-2.0 decreased by 52.2% compared with that of the original PA6 at a shear rate of 1000 s^{-1}, indicating that the addition of D_1 to PA6 resulted in excellent processability in industrial processing such as extrusion, injection molding, and spinning. In addition, the mechanical properties of chain-extended PA6 were also improved by the incorporation of D_1, especially the toughness. When the added amount of D_1 was 2.0 wt %, the elongation at break of the extended PA6 increased by 150.3%, and the notched impact strength increased by 69.7% compared with the elongation at break and notched impact strength of the original PA6. Moreover, D_1 showed a higher reactivity and a greater chain extension effect than the commercial chain extender ADR. These results suggest that the triepoxy chain extender (D_1) is suitable for preparing high-performance PA6 with excellent mechanical properties and processability in industrial production.

■ ASSOCIATED CONTENT

Supporting Information

The Supporting Information is available free of charge at https://pubs.acs.org/doi/10.1021/acs.iecr.0c02022.

Torque and the amino and carboxyl group content data of the original and extended PA6 and DSC and XRD data of the original and extended PA6 (PDF)

■ AUTHOR INFORMATION

Corresponding Authors

Shumei Liu − *School of Materials Science and Engineering, South China University of Technology, Guangzhou 510640, P. R. China; Key Laboratory of Guangdong High Property & Functional Polymer Materials, Guangzhou 510640, P. R. China;* orcid.org/0000-0003-3246-3811; Email: liusm@scut.edu.cn

Jianqing Zhao − *School of Materials Science and Engineering, South China University of Technology, Guangzhou 510640, P. R. China; Key Laboratory of Guangdong High Property & Functional Polymer Materials, Guangzhou 510640, P. R. China*; Email: psjqzhao@scut.edu.cn

Authors

Jianan Cai − *School of Materials Science and Engineering, South China University of Technology, Guangzhou 510640, P. R. China;* orcid.org/0000-0002-3211-1691

https://dx.doi.org/10.1021/acs.iecr.0c02022
Ind. Eng. Chem. Res. 2020, 59, 14334−14343

Zhipeng Liu − *School of Materials Science and Engineering, South China University of Technology, Guangzhou 510640, P. R. China*

Bo Cao − *School of Materials Science and Engineering, South China University of Technology, Guangzhou 510640, P. R. China*

Xiaoxiao Guan − *School of Materials Science and Engineering, South China University of Technology, Guangzhou 510640, P. R. China*

Complete contact information is available at: https://pubs.acs.org/10.1021/acs.iecr.0c02022

Author Contributions

The manuscript was written through the contribution of all authors. All authors have given approval to the final version of the manuscript.

Notes

The authors declare no competing financial interest.

■ ACKNOWLEDGMENTS

This research is supported by the Project for Science and Technology of Guangzhou (Grant no. 202007020001) and the Key Basic Research and Applied Basic Research Program of Guangdong Province (Grant no. 2019B1515120073).

■ REFERENCES

(1) Ozmen, S. C.; Ozkoc, G.; Serhatli, E. Thermal, Mechanical and Physical properties of Chain Extended Recycled Polyamide 6 via Reactive Extrusion: Effect of Chain Extender Types. *Polym. Degrad. Stab.* **2019**, *162*, 76−84.

(2) Tuna, B.; Benkreira, H. Reactive Extrusion of Polyamide 6 Using a Novel Chain Extender. *Polym. Eng. Sci.* **2019**, *59*, E25−E31.

(3) Lu, C. X.; Chen, L.; Ye, R. G.; Cai, X. F. Chain Extension of Polyamide 6 Using Bisoxazoline Coupling Agents. *J. Macromol. Sci., Part B: Phys.* **2008**, *47*, 986−999.

(4) Tuna, B.; Benkreira, H. Chain Extension of Recryled PA6. *Polym. Eng. Sci.* **2018**, *58*, 1037−1042.

(5) Bertani, R.; Boscolo-Boscoletto, A.; Dintcheva, N.; Ghedini, E.; Gleria, M.; la Mantia, F.; Pace, G.; Pannocchia, P.; Sassi, A.; Scaffaro, R.; Venzo, A. New Phosphazene-Based Chain Extenders Containing Allyl and Epoxide Groups. *Des. Monomers Polym.* **2003**, *6*, 245−266.

(6) Arayesh, H.; Ebrahimi, N. G.; Khaledi, B.; Esfahani, M. K. Introducing Four Different Branch Structures in PET by Reactive Processing–A Rheological Investigation. *J. Appl. Polym. Sci.* **2020**, 49243.

(7) Wirasaputra, A.; Zhao, J. Q.; Zhao, Y. M.; Liu, S. M.; Yuan, Y. C. Application of Bis(glycidyloxy)phenylphosphine Oxide as a Chain Extender for Polyamide-6. *RSC Adv.* **2015**, *5*, 31878−31885.

(8) Nofar, M.; Salehiyan, R.; Ray, S. S. Rheology of Poly (Lactic Acid)-Based Systems. *Polym. Rev.* **2019**, *59*, 465−509.

(9) Kruse, M.; Wang, P.; Shah, R. S.; Wagner, M. H. Analysis of High Melt-Strength Poly(ethylene terephthalate)Produced by Reactive Processing by Shear and Elongational Rheology. *Polym. Eng. Sci.* **2019**, *59*, 396−410.

(10) Yahyaee, N.; Javadi, A.; Garmabi, H.; Khak, A. Effect of Two-Step Chain Extension Using Joncryl and PMDA on the Rheological Properties of Poly (lactic acid). *Macromol. Mater. Eng.* **2020**, *305*, No. 1900423.

(11) Härth, M.; Kaschta, J.; Schubert, D. W. Shear and Elongational Flow Properties of Long-Chain Branched Poly(ethylene terephthalates) and Correlations to Their Molecular Structure. *Macromolecules* **2014**, *47*, 4471−4478.

(12) Rosu, R. F.; Shanks, R. A.; Bhattacharya, S. N. Dynamic Rheology of Branched Poly(ethylene terephthalate). *Polym. Int.* **2000**, *49*, 203−208.

(13) Xu, M. L.; Yan, H. C.; He, Q. J.; Wan, C.; Liu, T.; Zhao, L.; Park, C. B. Chain Extension of Polyamide 6 Using Multifunctional Chain Extenders and Reactive Extrusion for Melt Foaming. *Eur. Polym. J.* **2017**, *96*, 210−220.

(14) Rosu, R. F.; Shanks, R. A.; Bhattacharya, S. N. Shear Rheology and Thermal Properties of Linear and Branched Poly(ethylene terephthalate) Blends. *Polymer* **1999**, *40*, 5891−5898.

(15) Xanthos, M.; Young, M. W.; et al. Reactive Modification of Polyethylene Terephthalate with Polyepoxides. *Polym. Eng. Sci.* **2001**, *41*, 643−655.

(16) Li, X.; Yan, X. Y.; Yang, J.; Pan, H. W.; Gao, G. H.; Zhang, H. L.; Dong, L. S. Improvement of Compatibility and Mechanical Properties of the Poly(lactic acid)/Poly(butylene adipate-*co*-terephthalate) Blends and Films by Reactive Extrusion With Chain Extender. *Polym. Eng. Sci.* **2018**, *58*, 1868−1878.

(17) Kandpal, S.; Saxena, A. K. Studies on the Synthesis and Reaction of Silicone Oxirane Dendrimer and Their Thermal and Rheological Properties. *Eur. Polym. J.* **2014**, *58*, 115−124.

(18) Ghanbari, A.; Heuzey, M. C.; Carreau, P. J.; Ton-That, M. T. A Novel Approach to Control Thermal Degradation of PET/Organoclay Nanocomposites and Improve Clay Exfoliation. *Polymer* **2013**, *54*, 1361−1369.

(19) Najafi, N.; Heuzey, M. C.; Carreau, P. J.; Wood-Adams, P. M. Control of Thermal Degradation of Polylactide (PLA)-clay Nanocomposites Using Chain Extenders. *Polym. Degrad. Stab.* **2012**, *97*, 554−565.

(20) Shi, G.; Li, X. S.; Feng, Z. Y.; Wu, L. Y.; Ni, C. H. Preparation of Poly(N-buthyl methacrylate-co-glycidyl methacrylate) and Toughness Improvement for Powder Epoxy Resin E663. *Polym. Plast. Technol. Eng.* **2015**, *54*, 881−888.

(21) Waltz, J. E.; Taylor, G. B. Determination of the Molecular Weight of Nylon. *Anal. Chem.* **1947**, *19*, 448−450.

(22) Zhang, Y. J.; Zhang, C.; Li, H. Q.; Du, Z. J.; Li, C. J. Chain Extension of Poly(ethylene terephthalate) with Bisphenol-A Dicyanate. *J. Appl. Polym. Sci.* **2010**, *117*, 2003−2008.

(23) Wirasaputra, A.; Zheng, L. J.; Liu, S. M.; Yuan, Y. C.; Zhao, J. Q. High-Performance Flame-Retarded Polyamide-6 Composite Fabricated by Chain Extension. *Macromol. Mater. Eng.* **2016**, *301*, 614−624.

(24) Li, G.; Zhao, T.; Zhu, P. L.; He, Y. C.; Sun, R.; Lu, D. Q.; Wong, C. P. Structure-Property Relationships between Microscopic Filler Surface Chemistry and Macroscopic Rheological, Thermo-Mechanical, and Adhesive Performance of SiO_2 Filled Nanocomposite Underfills. *Composites, Part A* **2019**, *118*, 223−234.

(25) Zhao, T. H.; Wu, Y.; Li, Y. D.; Wang, M.; Zeng, J. B. High Performance and Thermal Processable Dicarboxylic Acid Cured Epoxidized Plant Oil Resins through Dynamic Vulcanization with Poly(lactic acid). *ACS Sustainable Chem. Eng.* **2017**, *5*, 1938−1947.

(26) Crowson, R. J.; Scott, A. J.; Saunders, D. W. Rheology of Short Glass Fiber-Reinforced Thermoplastics and Its Application to Injection Molding. III. Use of a High Shear Rate Capillary Rheometer in the Injection Molding Shear Rate Range. *Polym. Eng. Sci.* **1981**, *21*, 748−754.

(27) Cai, J. N.; Wirasaputra, A.; Zhu, Y. M.; Liu, S. M.; Zhou, Y. B.; Zhang, C. H.; Zhao, J. Q. The Flame Retardancy and Rheological Properties of PA6/MCA Modified by DOPO-Based Chain Extender. *RSC Adv.* **2017**, *7*, 19593−19603.

(28) Jahani, Y.; Ghetmiri, M.; Vaseghi, M. R. The Effects of Long Chain Branching of Polypropylene and Chain Extension of Poly-(ethylene terephthalate) on the Thermal Behavior, Rheology and Morphology of Their Blends. *RSC Adv.* **2015**, *5*, 21620−21628.

(29) Mei, Y. F.; Guo, B. H.; Xu, J. Detection of Long-Chain Branches in Polyethylene via Rheological Measurements. *Chin. Chem. Lett.* **2016**, *27*, 588−592.

(30) Boronat, T.; Segui, V. J.; Peydro, M. A.; Reig, M. J. Influence of Temperature and Shear Rate on the Rheology and Processability of Reprocessed ABS in Injection Molding Process. *J. Mater. Process. Technol.* **2009**, *209*, 2735−2745.

(31) Tian, J. H.; Yu, W.; Zhou, C. X. The Preparation and Rheology Characterization of Long Chain Branching Polypropylene. *Polymer* **2006**, *47*, 7962−7969.
(32) Chen, J.; Wei, W.; Qian, Q. R.; Xiao, L. R.; Liu, X. P.; Xu, J.; Huang, B. Q.; Chen, Q. H. The Structure and Properties of Long-Chain Branching Poly(trimethylene terephthalate). *Rheol. Acta* **2014**, *53*, 67−74.
(33) Liu, J.; Ye, L.; Zhao, X. W. Preparation of Long-Chain Branched Poly(ethylene terephthalate): Molecular Entanglement Structure and Toughening Mechanism. *Polym. Eng. Sci.* **2019**, *59*, 1190−1198.
(34) Wang, B.; Cavallo, D.; Zhang, X. L.; Zhang, B.; Chen, J. B. Evolution of Chain Entanglements Under Large Amplitude Oscillatory Shear Flow and Its Effect on Crystallization of Isotactic Polypropylene. *Polymer* **2020**, *186*, No. 121899.
(35) van Ruymbeke, E.; Stéphenne, V.; Daoust, D.; Godard, P.; Keunings, R.; Bailly, C. A Sensitive Method to Detect Very Low Levels of Long Chain Branching from the Molar Mass Distribution and Linear Viscoelastic Response. *J. Rheol.* **2005**, *49*, 1503−1520.
(36) Sun, Y. J.; Wu, L. B.; Bu, Z. Y.; Li, B. G.; Li, N. X.; Dai, J. M. Synthesis and Thermomechanical and Rheological Properties of Biodegradable Long-Chain Branched Poly(butylene succinate-co-butylene terephthalate) Copolyesters. *Ind. Eng. Chem. Res.* **2014**, *53*, 10380−10386.
(37) Chen, C. Q.; Ke, D. M.; Zheng, T. T.; He, G. J.; Cao, X. W.; et al. An Ultraviolet-Induced Reactive Extrusion to Control Chain Scission and Long-Chain Branching Reaction of Polylactide. *Ind. Eng. Chem. Res.* **2016**, *55*, 597−605.
(38) García-Franco, C. A.; Srinivas, S.; Lohse, D. J.; Brant, P. Similarities between Gelation and Long Chain Branching Viscoelastic Behavior. *Macromolecules* **2001**, *34*, 3115−3117.
(39) Robertson, C. G.; García-Franco, C. A.; Srinivas, S. Extent of Branching from Linear Viscoelasticity of Long-Chain-Branched Polymers. *J. Polym. Sci., Part B: Polym. Phys.* **2004**, *42*, 1671−1684.
(40) Zheng, X.; Ding, X. J.; Guan, J. P.; Gu, Y.; Su, Z. K.; Zhao, Y. M.; Tu, Y. F.; Li, X. H.; Li, Y. J.; Li, J. Y. Ionic Liquid-Grafted Polyamide 6 by Radiation-Induced Grafting: New Strategy to Prepare Covalently Bonded Ion-Containing Polymers and Their Application as Functional Fibers. *ACS Appl. Mater. Interfaces* **2019**, *11*, 5462−5475.
(41) Zhao, W. Y.; Huang, Y. J.; Liao, X.; Yang, Q. The Molecular Structure Characteristics of Long Chain Branched Polypropylene and Its Effects on Non-Isothermal Crystallization and Mechanical Properties. *Polymer* **2013**, *54*, 1455−1462.
(42) Bernadó, P.; Aleman, C.; Puiggali, J. Relative Stability between the α and γ Forms of Even Nylons Based on Group Contributions. *Eur. Polym. J.* **1999**, *35*, 835−847.
(43) Ho, J. C.; Wei, K. H. Induced $\gamma \rightarrow \alpha$ Crystal Transformation in Blends of Polyamide 6 and Liquid Crystalline Copolyester. *Macromolecules* **2000**, *33*, 5181−5186.
(44) Yan, X. L.; Imai, Y.; Shimamoto, D.; Hotta, Y. J. Relationship Study between Crystal Structure and Thermal/Mechanical Properties of Polyamide 6 Reinforced and Unreinforced by Carbon Fiber from Macro and Local View. *Polymer* **2014**, *55*, 6186−6194.
(45) Sang, L.; Wang, Y. K.; Chen, G. Y.; Liang, J. C.; Wei, Z. Y. A Comparative Study of the Crystalline Structure and Mechanical Properties of Carbon Fiber/Polyamide 6 Composites Enhanced with/without Silane Treatment. *RSC Adv.* **2016**, *6*, 107739−107747.
(46) Seo, Y. P.; Seo, Y. Effect of Molecular Structure Change on the Melt Rheological Properties of a Polyamide (Nylon 6). *ACS Omega* **2018**, *3*, 16549−16555.
(47) Deng, S. W.; Zhao, X. Z.; Huang, Y. M.; Han, X.; Liu, H. L.; Hu, Y. Deformation and Fracture of Polystyrene/Polypropylene Blends: A Simulation Study. *Polymer* **2011**, *52*, 5681−5694.
(48) Liang, Y.; Jensen, R. E.; Pappas, D. D.; Palmese, G. R. Toughening Vinyl Ester Networks with Polypropylene Meso-Fibers: Interface Modification and Composite Properties. *Polymer* **2011**, *52*, 510−518.

https://dx.doi.org/10.1021/acs.iecr.0c02022
Ind. Eng. Chem. Res. 2020, 59, 14334−14343